Queueing stability and CSI probing of a TDD wireless network with interference alignment

Matha Deghel, Mohamad Assaad, Merouane Debbah

Queueing Stability and CSI Probing of a TDD Wireless Network with Interference Alignment

Matha Deghel[⋆,◇], Mohamad Assaad[⋆] and Merouane Debbah[◇,†]

[⋆]Department of Telecommunications, CentraleSupélec, 91192, Gif-sur-Yvette, France
[◇]Large Networks and Systems Group (LANEAS), CentraleSupélec, France
[†]Mathematical and Algorithmic Sciences Lab, Huawei France R&D, Paris, France
{matha.deghel, mohamad.assaad, merouane.debbah}@supelec.fr

***Abstract*—This paper characterizes the performance of IA technique taking into account the dynamic traffic pattern and the probing/feedback cost. We consider a TDD system where transmitters acquire their CSI (Channel State Information) by decoding the pilot sequences sent by the receivers. Since global CSI knowledge is required for IA, the transmitters have also to exchange their estimated CSIs over a backhaul of limited capacity. Under this setting, we characterize in this paper the stability region of the system and provide a probing algorithm that achieves the max stability region. In addition, we compare the stability region of IA to the one achieved by a TDMA system where each transmitter applies a simple ZF (Zero Forcing technique).**

I. Introduction

One of the key issue in wireless communication systems is the interference which is caused by a large number of users communicating on the same channel. Interference alignment (IA) is introduced in [1] as one of the most efficient interference management techniques. It is based on the concept of aligning the interferences in a reduced dimensional subspace, so that the desired signal can be transmitted with less interference in a larger subspace. One disadvantage of IA is that it requires global channel state information (CSI) at each of the transmitting nodes, which is difficult to obtain in practical systems. Therefore, IA under limited feedback was studied and several quantization schemes were proposed, in order to aid the transmitters to acquire CSI knowledge from receivers and then to share it between each other [2]–[6].

Another important factor to consider is the CSI acquisition (probing) cost. We consider a system under Time-Division Duplex (TDD) mode where users send training sequences in the uplink so that the transmitters can estimate their channels. This scheme uses orthogonal sequences among the users, so their lengths are proportional to the number of active users in the system. It means that after acquiring the CSI of L users, the throughput is multiplied by $1-L\theta$, where θ is the fraction of time that takes the CSI acquisition of one user [7].

From the above, it can be seen that the more L is large, the more the acquisition process consumes a larger fraction of time and hence leaves a smaller fraction for transmission. Thus, it is important to focus on the tradeoff between having a large number of active transmitter-receiver pairs (which means a high probing cost but many pairs can communicate simultaneously) and having small L (a small probing cost but few pairs can communicate simultaneously) [8]. In the end, the system should determine what pairs to schedule at each time slot. To provide an answer to this question, one major way is to use opportunistic scheduling. It is based on the principle of scheduling users based on their channel states and queue lengths, which can ensure the stability of the system. Many scheduling strategies were proposed under various traffic and network scenarios. In [9], the authors have proposed the max-weight scheduling policy and have shown its optimality. Scheduling with limited CSI information have been analyzed in [7]. Furthermore, the impact of delay on the stability has been analyzed under zero forcing SDMA and limited feedback case [10]. Finally, probing cost and scheduling were jointly investigated in [8].

The context here is different from the aformentioned work. We consider a network where multiple transmitter-receiver pairs operate in TDD mode and apply the IA technique under backhaul links of limited capacity. The CSIs are then obtained by decoding the pilots sent by the receivers and then the transmitters exchange their estimated CSIs over the backhaul. A major contribution of this work is the precise characterization of the stability region of the system under all the considerations mentioned before. Furthermore, we provide an algorithm that selects the users that must send their pilots in each time slot (i.e. it schedules the active pairs). Another main contribution is the comparison between IA and TDMA-ZF (zero forcing) techniques in terms of stability regions.

The rest of this paper is organized as follows. The system model is presented in Section II. In Section III, the stability of the system is analyzed and the comparison between IA and ZF is provided. Section IV is dedicated to numerical results and relevant discussions. Finally, Section V concludes the paper.

Notation: Boldface uppercase symbols (i.e., $\mathbf{A}$) represent matrices whereas lowercases (i.e., $\mathbf{a}$) are used for vectors. $\mathbf{a}^*$ denotes the conjugate transpose of $\mathbf{a}$. The symbol $\mathbf{I}$ denotes square identity matrix. $\otimes$ is the Kronecker product. $|.|$ indicates the absolute value, $||.||_1$ and $||.||$ are used for the norm of first and second degree, respectively.

II. System Model

We consider the MIMO interference channel with N transmitter-receiver pairs shown in Fig. 1. For simplicity of exposition, we consider a network where all transmitters and all receivers (users) are equipped with N_t and N_r antennas, respectively. Each transmitter communicates with its intended

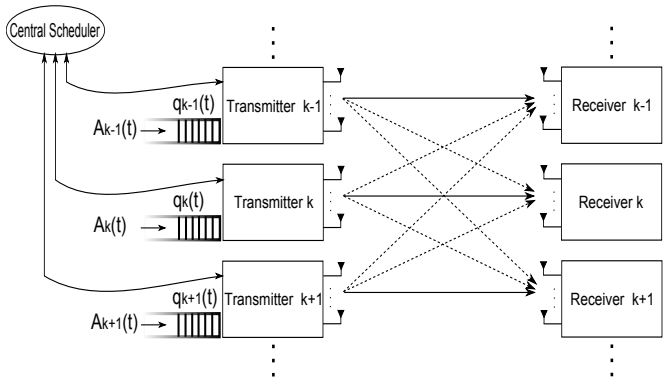

Figure 1: MIMO interference network with limited backhaul.

user via $d \leq \min(N_t, N_r)$ independent data streams, and interferes with all other unintended users. We assume that time is slotted. As we will see later on, only a subset $\mathcal{L}(t)$ (of cardinality $L(t)$) of pairs are active at each time slot, with $L(t) \leq N$. For notational convenience we will drop the notation for dependence on t and L.

Given this channel model, the received signal at active user k can be expressed as

$$\mathbf{y}_k = \sqrt{\frac{P}{d}}\mathbf{H}_{kk}\sum_{j=1}^{d}\mathbf{v}_k^j x_k^j + \sum_{\substack{i=1\\ i\neq k}}^{L}\sqrt{\frac{P}{d}}\mathbf{H}_{ki}\sum_{j=1}^{d}\mathbf{v}_i^j x_i^j + \mathbf{z}_k \quad (1)$$

where $\mathbf{y}_k$ is the $N_r \times 1$ received signal vector, $\mathbf{z}_k$ is the additive white Gaussian noise with zero mean and covariance matrix $\sigma^2\mathbf{I}_{N_r}$, $\mathbf{H}_{ki}$ is the $N_r \times N_t$ channel matrix between transmitter i and receiver k with independent and identically distributed (i.i.d.) zero mean and unit variance complex Gaussian entries, P is the total power at each transmitting node, which is equally allocated among its data streams, x_i^j represents the j-th data stream from transmitter i, and $\mathbf{v}_i^j$ is the corresponding $N_t \times 1$ precoding vector of unit norm. Let $\alpha = \frac{P}{d}$.

A. Interference Alignment Technique

For tractability, we restrict ourselves to a per-stream zero-forcing receiver. In such a system, receiver k uses the $N_r \times 1$ *combiner* vector $\mathbf{u}_k^m$ of unit norm to detect its m-th stream, which gives

$$\begin{aligned}\hat{x}_k^m &= (\mathbf{u}_k^m)^* \mathbf{y}_k \\ &= \overbrace{\sqrt{\alpha}\,(\mathbf{u}_k^m)^*\mathbf{H}_{kk}\mathbf{v}_k^m x_k^m}^{\text{desired signal}} + \overbrace{\sqrt{\alpha}\sum_{\substack{j=1\\ j\neq m}}^{d}(\mathbf{u}_k^m)^*\mathbf{H}_{kk}\mathbf{v}_k^j x_k^j}^{\text{inter-stream interference (ISI)}} \\ &\quad + \overbrace{\sqrt{\alpha}\sum_{\substack{i=1\\ i\neq k}}^{L}\sum_{j=1}^{d}(\mathbf{u}_k^m)^*\mathbf{H}_{ki}\mathbf{v}_i^j x_i^j}^{\text{inter-user interference (IUI)}} + \overbrace{(\mathbf{u}_k^m)^*\mathbf{z}_k}^{\text{noise}}. \end{aligned} \quad (2)$$

In order to mitigate the interferences in (2), we can design the set of combiner and precoder vectors such that

$$(\mathbf{u}_k^m)^*\mathbf{H}_{ki}\mathbf{v}_i^j = 0, \qquad \forall (k,m) \neq (i,j). \quad (3)$$

Note that the above conditions are those of a *perfect interference alignment*. In other words, suppose that all the transmitting nodes have perfect global CSI and each receiver obtains a perfect version of its corresponding combiner vector, ISI and IUI can be suppressed completely. However, obtaining the perfect global CSI at the transmitters is not always practical due to the fact that backhaul links, which connect transmitters to each other, are of limited capacity. The condition on the feasibility of IA is given by the following remark.

Remark 1. *To ensure the feasibility of the interference alignment problem, we have to respect the condition (given in [11]) $N_t + N_r \geq d(L+1)$. Without loss of generality, we assume that the maximal number N of pairs satisfies this condition.*

In the following, the CSI sharing mechanism is detailed.

B. CSIT Sharing Over Limited Capacity Backhaul Links

We use a TDD transmission strategy which enables the transmitters to estimate their channels toward different receivers by exploiting the reciprocity of the wireless channel, meaning that the i-th transmitter estimates the channels $\mathbf{H}_{ki}$, for $k = 1, ..., L$, $k \neq i$. This set of estimated channels is denoted by *local CSI* of transmitter i. We assume that each transmitter estimates perfectly its local CSI. But, as mentioned earlier, global CSI is required at each transmitting node in order to design IA vectors. For this purpose, active transmitting nodes need to share their local knowledge between each other, and this can be done via backhaul links which are, practically, of limited capacity.

We consider the topology of CSI sharing shown in Fig. 1, where all the transmitters are connected to a central scheduler via backhaul links of finite capacity, which serves as a way for connecting transmitters to each other. Since backhaul links are of limited capacity, codebook-based quantization is an effective way to reduce the huge amount of information exchange needed for CSI sharing. In detail, let $\mathbf{h}_{ki}$ denote the vectorization of the channel matrix $\mathbf{H}_{ki}$, then transmitter i selects an optimal codeword from a predetermined codebook $\mathcal{CB} = \left\{\hat{\mathbf{h}}_{ki}^1, ..., \hat{\mathbf{h}}_{ki}^{2^B}\right\}$ of size 2^B according to the following: $n_o = \arg\max_{1\leq n\leq 2^B}\left|\tilde{\mathbf{h}}_{ki}^*\hat{\mathbf{h}}_{ki}^n\right|^2$, where $\tilde{\mathbf{h}}_{ki} = \mathbf{h}_{ki}/\left\|\mathbf{h}_{ki}\right\|$ is the channel direction vector and B is the number of bits.
After that transmitter i quantizes all the matrices of its local CSI by computing their corresponding optimal indexes, it sends these indexes to all other active transmitters which share the same codebook, allowing these transmitters to reconstruct the quantized local CSI of transmitter i.

To define the error e_{ki} resulting from each quantization process, we adopt the same model as in [2], [10]. Based on this, e_{ki} can be defined as $e_{ki} = 1 - \left(\left|\hat{\mathbf{h}}_{ki}^*\mathbf{h}_{ki}\right|^2 / \left\|\mathbf{h}_{ki}\right\|^2\right)$, and its corresponding cumulative distribution function (CDF) is given by: $\Pr(e_{ki} \leq \varepsilon) = 2^B\varepsilon^Q, 0 \leq \varepsilon \leq 2^{-\frac{B}{Q}}$, where $Q = N_tN_r - 1$.

C. Rate model

As explained in the previous section, each transmitter designs its IA vectors based on a perfect version of its local CSI and an imperfect (quantized) version of local CSI of

other transmitters. For this reason, the IA technique is able to completely cancel the ISI, but not the IUI. Thus, under such observation and using the results in [12], the SINR for stream m at receiver k can be written as

$$\gamma_k^m = \frac{\alpha \left|(\hat{\mathbf{u}}_k^m)^* \mathbf{H}_{kk} \hat{\mathbf{v}}_k^m\right|^2}{\sigma^2 + \alpha \sum\limits_{\substack{i=1 \\ i\neq k}}^{L} \|\mathbf{h}_{ki}\|^2 e_{ki} \sum\limits_{j=1}^{d} \left|(\mathbf{w}_{ki})^* \mathbf{T}_{k,i}^{m,j}\right|^2}, \quad (4)$$

where $\mathbf{w}_{ki}$ is a unit norm vector isotropically distributed in the null space of $\hat{\mathbf{h}}_{ki}$, $\mathbf{T}_{k,i}^{m,j} = \hat{\mathbf{v}}_i^j \otimes (\hat{\mathbf{u}}_k^m)^*$, $\hat{\mathbf{v}}_k^m$ and $\hat{\mathbf{u}}_k^m$ are the combining and precoding vectors, respectively, designed based on the available global CSI at transmitter k.

As alluded earlier, only a subset $\mathcal{L}$ (with $|\mathcal{L}| = L$) of users is scheduled at a time. Note that under the considered system model, it can be easily noticed that the rate of an active user depends only on the cardinality L of $\mathcal{L}$ and not the subset $\mathcal{L}$ itself. We now explain some useful points which are adopted in the rate model.

For a fixed modulation and coding scheme and with interference treated as noise, a well accepted model for transmissions is that they succeed if the SINR exceeds a certain threshold τ. Thus, the average rate for active user k can be written in function of the transmission success probability conditioned on the number of active pairs as $R\mathbb{P}(\gamma_k^m \geq \tau \mid L)$, where R is the assigned transmission rate per user [10].

Channel acquisition cost is not negligible and should be considered. For that, we assume that acquiring the CSI of one user takes fraction θ of the slot, and then the rate expression becomes $(1 - L\theta)R\mathbb{P}(\gamma_k^m \geq \tau \mid L)$.

D. Queue Dynamics and Scheduling

For each user, we assume that the incoming data is stored in a respective queue (buffer) until transmission and we denote by $\mathbf{q}(t) = [q_1(t), ..., q_N(t)]$ the queue length vector. Let $\mathbf{A}(t) = [A_1(t), ..., A_N(t)]$ denote the vector of number of bits arriving in the buffers in time slot t, which is an i.i.d. in time process, independent across users and with $A_k(t) < a_{max}$. The mean arrival rate for receiver k is denoted by $a_k = \mathbb{E}[A_k(t)]$. We designate by $\mathbf{B}(t) = [B_1(t), ..., B_N(t)]$ the vector of number of bits served at time slot t with $B_k(t) < b_{max}$. Note that, for each user, this number can be given by the minimum between the corresponding rate and the queue length.

In each slot, the central scheduler selects a subset $\mathcal{L}$ (recall that $|\mathcal{L}| = L$) of users that must send their pilots so that their corresponding transmitters can estimate the CSIs. Then, these scheduled transmitter-receiver pairs will be active for transmission. As we will see later, the scheduling decision depends on the average rate and the queue lengths of all N pairs. One can notice that the average rate expression depends on $L\theta$ which represents the probing cost. Thus, if we select a large number of pairs L for transmission, many pairs can communicate (i.e. this will leave a small fraction of time for transmission) but a high CSI acquisition cost ($L\theta$) is needed. On the other hand, a small L requires a low acquisition cost, but, at the same time, it allows a few number of simultaneous transmissions. The scheduling policy, i.e. scheduling decision, can be represented by an indicator vector $\mathbf{s} \in \mathbb{Z}^N$ where the kth component is equal to 1 if the kth queue (pair) is scheduled and equal to 0 otherwise. We denote $\mathcal{S}$ as the set of all possible vectors $\mathbf{s}$, thus the cardinality of this set is equal to $|\mathcal{S}| = 2^N$.

In this work, the focus will be mainly on the stability of the system. To this end, we give the following definition:

Definition 1. *The stability region can be defined as the set of arrival rate vectors for which all the queues of all users are strongly stable. The condition for strong stability can be expressed as*

$$\limsup_{T\to\infty} \frac{1}{T} \sum_{t=0}^{T-1} \mathbb{E}[q_k(t)] < \infty, \forall k \in \{1, ..., N\}. \quad (5)$$

Note that a scheduling policy that stabilizes the system for all this set of arrivals is called throughput optimal. Under a policy Δ, the queue length dynamics can be given by

$$\mathbf{q}^{(\Delta)}(t+1) = \max\left\{\mathbf{q}^{(\Delta)}(t) + \mathbf{A}(t) - \mathbf{B}^{(\Delta)}(t), \mathbf{0}\right\}, \quad (6)$$

where the max operator is component-wise.

III. Stability Analysis of IA

For ease of exposition, we restrict ourselves to the case with one modulation (see Section II). Essentially, a similar analysis can be done for the case with multiple modulations, which is given in Appendix G.

A. Average Transmission Rate

In this subsection, we are interested in deriving the average rate per user and the total average rate of the system. In addition, we provide an analysis of the behavior of these rate functions with the variation of the number of active users.

As explained in the previous section, if $\mathcal{L}$ is the subset of scheduled users, the average transmission rate per active user is given by $(1 - L\theta)R\mathbb{P}(\gamma_k^m \geq \tau \mid L)$ since the average rate depends only on the cardinality L of subset $\mathcal{L}$. Relying on the recent result in [12] where the transmission success probability is derived, we have that the *average transmission rate* for an active user can be given by

$$r = Re^{-\frac{\sigma^2\tau}{\alpha}}(1 - L\theta)F^{L-1}, \quad (7)$$

in which $F = \kappa_1^{-Q}\, {}_2F_1(\beta_2, Q; \beta_1 + \beta_2; \kappa_2^{-1})$, where ${}_2F_1$ is the hypergeometric function, $\kappa_1 = (1 + \frac{d\tau}{2^{\frac{B}{Q}}})$, $\kappa_2 = (1 + \frac{2^{\frac{B}{Q}}}{d\tau})$, $\beta_1 = \frac{(Q+1)d}{Q} - \frac{1}{Q}$ and $\beta_2 = (Q-1)\beta_1$.

Notice that this rate is the same for all the active users for our system model. Consequently, the *total average transmission rate* of the system is given by

$$r_T = Re^{-\frac{\sigma^2\tau}{\alpha}} L(1 - L\theta)F^{L-1}. \quad (8)$$

The variation of these rate functions with L is described by the following lemma.

Lemma 1. *Given a number of users to be scheduled, L, the average transmission rate is a decreasing function with L, whereas the total average transmission rate function reaches its maximum at $L_1 < \frac{1}{2\theta}$, where L_1 is given by*

$$L_1 = \frac{\frac{1}{\theta} - \frac{2}{\log F} - \sqrt{\left(\frac{2}{\log F} - \frac{1}{\theta}\right)^2 + \frac{4}{\theta \log F}}}{2}. \quad (9)$$

Proof. The proof is provided in Appendix A. □

Remark 2. *One limitation on the optimal number of pairs, which is satisfied in our case, is that it should be lower than the factor* $\frac{1}{\theta}$. *This comes from the fact that* $1 - L\theta < 1$.

From (9) we can notice that L_1 is in general a real value. Since it represents a number of users, we can find the best and nearest integer to L_1, i.e. best in terms of maximizing the total average rate function. We denote this integer by L_m and we assume that $N > L_m$.

B. Stability Analysis

After presenting results on the average rate function, we now provide a precise characterization of the stability region of the adopted system. Before proceeding in the analysis, we define the subset S_L as the following $S_L = \{\mathbf{s} : \|\mathbf{s}\|_1 = L\}$, where $\mathbf{s} \in \mathbb{Z}^N$ is the vector whose coordinates take values 0 or 1 (see Section II). In addition, we denote r_L and $r(L)$ as an equivalent representations of the average rate r (since r depends on L). Let G_L a subset defined as $G_L = \{r_L\mathbf{s}, \forall \mathbf{s} \in S_L\}$. For these subsets, we define the set $\mathcal{R}$ and its complementary set $\bar{\mathcal{R}}$ as $\mathcal{R} = \{G_1, G_2, ..., G_{L_m}\}$ and $\bar{\mathcal{R}} = \{G_{L_m+1}, ..., G_N\}$. Notice that $|\mathcal{R}| + |\bar{\mathcal{R}}| = |\mathcal{S}|$. Under these considerations, we can state the following lemma which is useful to characterize the stability region of the system.

Lemma 2. *Each point in* $\bar{\mathcal{R}}$ *is inside the convex hull of* $\mathcal{R}$.

Proof. The detailed proof can be found in Appendix B. □

Now, we have all the materials to characterize the stability region of the system, which is given by the following theorem.

Theorem 1. *The stability region of the adopted system can be characterized as*

$$\Lambda_c = \mathcal{CH}\left\{G_1, G_2, ..., G_{L_m}\right\} = \mathcal{CH}\left\{\mathcal{R}\right\}, \tag{10}$$

where $\mathcal{CH}$ *represents the convex hull.*

Proof. The proof is provided in Appendix C. □

Unlike classical results in which the stability region is given by the convex hull over all possible decisions, here the characterization is more precise and is defined by the decision subsets S_L for all $L \leq L_m$. In addition, this theorem provides an exact specification of the corner points (vertices) of the stability region (it means that this region is defined by the set $\mathcal{R}$ and not the whole space).

In order to choose the users who will send their pilots, we use the following scheduling policy

$$\Delta^* : \mathcal{L}(t) = \arg\max_{\mathbf{s}\in\mathcal{S}} \left\{r(\|\mathbf{s}\|_1)\, \mathbf{s} \cdot \mathbf{q}(t)\right\}, \tag{11}$$

where $\|\mathbf{s}\|_1$ gives the number of '1' coordinates in $\mathbf{s}$ (or equivalently, the number of active pairs). Note that these non-zero coordinates precise what pairs to schedule. One can remark that unlike the standard max-weight, the policy in our case depends on the average rate and not the instantaneous one. For the proposed policy, we have the following proposition.

Proposition 1. *The scheduling policy* Δ^* *is throughput optimal. In other words,* Δ^* *stabilizes the system for every arrival rate vector* $\mathbf{a} \in \Lambda_c$.

Proof. To prove optimality, we use Foster's theorem [13]. We present the proof in Appendix D for completeness. □

Notice that implementing Δ^* for large N is of high computational complexity (CC). For this, we analyze the CC of this policy and we propose an algorithm which reduces considerably this complexity. This is provided in Appendix E.

C. Compare IA to Zero Forcing

In this subsection, we characterize the stability region of the case when we use zero forcing (ZF) technique with time division multiple access (TDMA) instead of interference alignment. After that, we investigate which one of these two techniques outperforms the other in terms of stability.

In the case where we apply TDMA-ZF technique, there is only one active pair at a time, so the average rate of this pair can be given by [10]

$$\begin{aligned} r_{\text{zf}} &= R(1-\theta)\mathbb{P}(\gamma_k^m \geq \tau) \\ &= R(1-\theta)\left(1 - F_{\chi^2_{2(N_r-N_t+1)}}\left(\frac{\tau}{snr}\right)\right), \end{aligned} \tag{12}$$

where $F_{\chi^2_{2(N_r-N_t+1)}}$ is the cumulative density function of $\chi^2_{2(N_r-N_t+1)}$ and $snr = \frac{\alpha}{\sigma^2}$. Under the above considerations, the stability region for TDMA-ZF can be described as follows.

Proposition 2. *If we apply TDMA-ZF technique, the stability region of the corresponding system can be given by*

$$\Lambda_{zf} = \mathcal{CH}\left\{J_1\right\}, \tag{13}$$

where $J_1 = \{r_{zf}\mathbf{s}, \forall \mathbf{s} \in S_1\}$.

This proposition results from the fact that only one pair is active at a time, thus only subset S_1 is considered since it contains all the possible combinations of choosing one pair.

To compare the performance of IA and TDMA-ZF techniques, we adopt the following reasoning: we investigate if there exists an L (with $L \leq L_m$) such that the stability region for IA (defined in Theorem 1) surpasses, even partially, the stability region for TDMA-ZF given in the previous proposition. This leads to the following theorem:

Theorem 2. *In terms of stability, interference alignment can outperform TDMA zero forcing if there exists a number* L *(with* $1 \leq L \leq L_m$*) such that* $Lr_L > r_{zf}$. *If this condition is not satisfied, then it is better to use TDMA zero forcing technique.*

Proof. Please refer to Appendix F for the proof. □

This theorem provides a kind of rule which allows the system deciding if the transmission should be done with TDMA-ZF or IA technique. This decision is made based on the existence (or not) of a number of pairs L such that $Lr_L > r_{\text{zf}}$. Specifically, if the first condition in Theorem 2 is satisfied, it may be beneficial to use the IA technique since we have a part of its stability region that surpasses the stability region of TDMA-ZF (given by Λ_{zf}). On the other hand, if this condition is not satisfied, then the stability region of IA is entirely inside Λ_{zf}, and thus it is better to use TDMA-ZF technique.

IV. Numerical Results

In this section we present our numerical results. We consider a system where the number of antennas $N_t = N_r = 10$, SNR $= \frac{P}{\sigma^2} = 10$ dB, $d = 2$, $\theta = 0.01$, $\tau = 1$. We take $N = 9$ and we assume that all users have Poisson incoming traffic with the same average arrival rates as $a_k = a$. We set the slot duration to $T_s = 1$ ms and we consider a bandwidth $BW = 10$ MHz. Therefore, the assigned transmission rate per (active) user can be given by $R = d\,BW \log_2(1+\tau)$ bits/s = 20 Mbits/s = 20 Kbits/slot. In this section we include the path loss of the direct and cross links. Even though in practice all the path loss coefficients are different, we consider in this section a very special case that can provide more insights on the comparison between IA and TDMA-ZF. In fact, we want to show the impact of the cross links on the performance of these 2 schemes. In order to have more insightful results, we consider that all the direct links have a path loss coefficient of 1 and all the cross links have a path loss of ζ (with $\zeta \leq 1$). This allows us to see, with respect to ζ, when IA performs better than TDMA-ZF and vice versa.

To show the stability performance of the system, we plot the total average queue length given by $\frac{1}{M}\sum_{t=0}^{M-1}\sum_{k=1}^{N} q_k(t)$ for different values of a, where each simulation takes M timeslots. We set $M = 10^5$. Note that the point where the total average queue length function increases very steeply is the point at which the system becomes unstable.

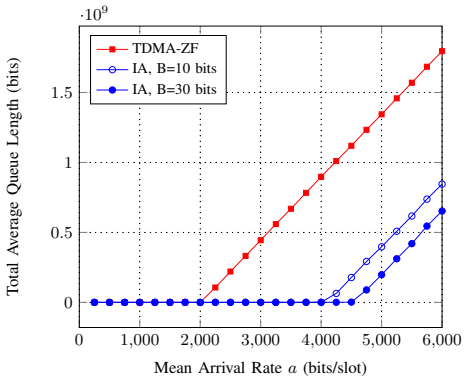

Figure 2: Total average queue length vs. mean arrival rate a. $\zeta = 0.1$.

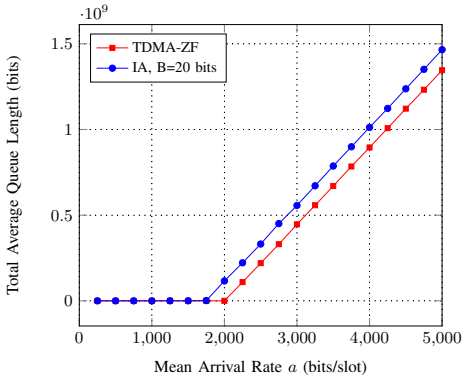

Figure 3: Total average queue length vs. mean arrival rate a. $\zeta = 0.3$.

Fig. 2 shows that IA gives better performances when we increase the number of bits. This is due to the fact that the more the quantization is precise, the more we achieve higher rates which implies better stability performance.

From Fig. 2 and 3, we can see that TDMA-ZF outperforms IA when the interference impact is high (for instance $\zeta = 0.3$), whereas we obtain the converse for less interfering system ($\zeta = 0.1$). This is due to the fact that when ζ increases the performance of IA is more sensitive to the number of quantization bits B. It is worth mentioning that there exist other parameters that affect this comparison such as, for example, the number of antennas, the threshold τ, the backhaul capacity which specifies B and so on. For these comparisons, one last thing we should mention is that for IA the CSI sharing process over the backhaul costs $L^2(L-1)B$ bits per transmission, while no such cost is needed when using TDMA-ZF technique.

V. Conclusion

In this paper, we characterized the stability region for IA in a general MIMO interference network under TDD mode with limited backaul capacity and taking into account the probing cost. We provided an optimal scheduling algorithm that achieves this region. We compared IA and TDMA-ZF techniques in terms of stability region and provided a condition for which TDMA-ZF outperforms IA.

References

[1] V. R. Cadambe and S. A. Jafar, "Interference alignment and degrees of freedom of the k-user interference channel," *IEEE Trans. Inform. Theory*, vol. 54, no. 8, pp. 3425–3441, August 2008.

[2] X. Chen and C. Yuen, "Performance analysis and optimization for interference alignment over MIMO interference channels with limited feedback," *arXiv preprint arXiv:1402.0295*, 2014.

[3] O. E. Ayach and R. W. Heath, "Interference alignment with analog channel state feedback," *IEEE Trans. Wireless Commun.*, vol. 11, no. 2, pp. 626–636, February 2012.

[4] R. T. Krishnamachari and M. K. Varanasi, "Interference alignment under limited feedback for MIMO interference channels," *IEEE Trans. Signal Processing*, vol. 61, no. 15, pp. 3908–3917, August 2013.

[5] M. Rezaee, M. Guillaud, and F. Lindqvist, "CSIT sharing over finite capacity backhaul for spatial interference alignment," in *IEEE International Symposium on Information Theory Proceedings (ISIT'13)*. IEEE, July 2013, pp. 569–573.

[6] S.-H. Park, O. Simeone, O. Sahin, and S. Shamai, "Performance evaluation of multiterminal backhaul compression for cloud radio access networks," in *48th Annual Conference on Information Sciences and Systems (CISS'14)*. IEEE, March 2014, pp. 1–6.

[7] P. Chaporkar, A. Proutiere, H. Asnani, and A. Karandikar, "Scheduling with limited information in wireless systems," in *Proceedings of the tenth ACM international symposium on Mobile ad hoc networking and computing*, ser. MobiHoc '09. New York, NY, USA: ACM, 2009, pp. 75–84.

[8] A. Destounis, M. Assaad, M. Debbah, and B. Sayadi, "Traffic-aware training and scheduling for the 2-user MISO broadcast channel," in *2014 IEEE International Symposium on Information Theory (ISIT)*, June 2014, pp. 1376–1380.

[9] L. Tassiulas and A. Ephremides, "Dynamic server allocation to parallel queues with randomly varying connectivity," *IEEE Trans. Inform. Theory*, vol. 39, no. 2, pp. 466–478, Mar 1993.

[10] K. Huang and V. Lau, "Stability and delay of zero-forcing SDMA with limited feedback," *IEEE Trans. Inform. Theory*, vol. 58, no. 10, pp. 6499–6514, Oct 2012.

[11] C. M. Yetis, T. Gou, S. A. Jafar, and A. H. Kayran, "On feasibility of interference alignment in MIMO interference networks," *IEEE Trans. Signal Processing*, vol. 58, no. 9, pp. 4771–4782, September 2010.

[12] M. Deghel, M. Assaad, and M. Debbah, "System performance of interference alignment under TDD mode with limited backhaul capacity," in *IEEE International Conference on Communications (ICC'2015)*, London, UK, Submitted, [Online] http://goo.gl/NhGBKk.

[13] G. Fayolle, V. A. Malyshev, and M. V. Menshikov, *Topics in the Constructive Theory of Countable Markov Chains*. Cambridge University Press, 1995, cambridge Books Online. [Online]. Available: http://dx.doi.org/10.1017/CBO9780511984020

APPENDIX A
PROOF OF LEMMA 1

We start the proof by first showing that $r(L)$ decreases with L. The first derivative of this rate function is given by

$$\frac{dr}{dL} = Re^{-\frac{\sigma^2\tau}{\alpha}} F^{L-1}(-\theta + (1-L\theta)\log F) \tag{14}$$

Since we have $L < \frac{1}{\theta}$ and $\log F < 0$, the first derivative is negative and so r decreases with L.
To analyze the variation of $r_T(L)$ we need to compute the first and second derivatives of this function (w.r.t. L), which help us determine the optimal number of pairs, such as

$$\frac{dr_T}{dL} = Re^{-\frac{\sigma^2\tau}{\alpha}} F^{L-1}\left(1 - 2L\theta + (L - L^2\theta)\log F\right) \tag{15}$$

$$\frac{d^2 r_T}{dL^2} = Re^{-\frac{\sigma^2\tau}{\alpha}} F^{L-1} \times \left(-2\theta + 2(1-2L\theta)\log F + (L - L^2\theta)(\log F)^2\right) \tag{16}$$

Putting the first and second derivatives equal to zero gives, respectively,

$$L_{\frac{2}{1}} = \frac{\frac{1}{\theta} - \frac{2}{\log F} \pm \sqrt{\left(\frac{2}{\log F} - \frac{1}{\theta}\right)^2 + \frac{4}{\theta \log F}}}{2} \tag{17}$$

$$L_{\frac{4}{3}} = \frac{-4 + \frac{\log F}{\theta} \pm \sqrt{\left(4 - \frac{\log F}{\theta}\right)^2 + \frac{8}{\theta} - \frac{8}{\log F}}}{2} \tag{18}$$

Note that $\log F < 0$ and $\left(\frac{2}{\log F} - \frac{1}{\theta}\right)^2 + \frac{4}{\theta \log F} = \frac{1}{\theta^2} + \frac{4}{(\log F)^2}$.
We now study the results in (17) and (18).
Since $\frac{1}{\theta} - \frac{2}{\log F} > \sqrt{\frac{1}{\theta^2} + \frac{4}{(\log F)^2}}$, it results that $L_2 > \sqrt{\frac{1}{\theta^2} + \frac{4}{(\log F)^2}} > \frac{1}{\theta}$, which implies that L_2 is to reject due to the constraint $L < \frac{1}{\theta}$. Moreover, we have that $L_1 < \frac{1}{2\theta} - \frac{2}{2\log F} - \frac{1}{2}\sqrt{\frac{4}{(\log F)^2}} = \frac{1}{2\theta}$. For the expressions in (18), we can see that $L_3 < 0$ and that $L_4 > 0$.
Based on the above observations, the variation of $r_T(L)$ can be described as follows: $r_T(L)$ increases for $L < L_1$, decreases between L_1 and L_2 and then increases for $L > L_2$. For the sake of brevity, we omit the proof of this part.
Therefore, the total average rate function r_T reaches its maximum at L_1.

As mentioned in Section III, L_1 is in general a real value, thus we need to find the best and nearest integer (denoted by L_m) to L_1. To clarify how L_m is selected, we give the following simple procedure:

1) Calculate L_1 using (9).
2) Let $L_{11} = \lfloor L_1 \rfloor$ and $L_{12} = \lceil L_1 \rceil$, i.e. the largest previous and the smallest following integer of L_1, respectively.
3) If $r_T(L_{12}) \geq r_T(L_{11})$, then $L_m = L_{12}$; otherwise put $L_m = L_{11}$.

APPENDIX B
PROOF OF LEMMA 2

We first give and prove the following lemma which will help us in the proof of Lemma 2.

Lemma 3. *Each point (vector) in S_{L+1} can be written as $\frac{L+1}{L}\times$ some point in the convex hull of S_L.*

Proof. We start the proof by calculating the number of vectors in S_L that have the same L non-zero ('1') coordinates as the vector $\mathbf{s}_{i,L+1} \in S_{L+1}$. This number can be interpreted as the combination of $L+1$ elements taken L at a time without repetition, which can be written as $\binom{L+1}{L} = \frac{(L+1)!}{L!(L+1-L)!} = L+1$.
Thus, we have $L+1$ elements from S_L that if we take them in a specific convex combination, we get a point on the same line (from the origin) as that of $\mathbf{s}_{i,L+1}$. This can be represented by

$$\sum_{j=1}^{L+1} \delta_j \mathbf{s}_{j,L} \equiv \mathbf{s}_{i,L+1}, \tag{19}$$

where $\equiv$ is a notation used to say that these two points are on the same line, $\sum_{j=1}^{L+1} \delta_j = 1$ and $\delta_j > 0$.
Let us suppose that all the $\delta_j = \frac{1}{L+1}$, which satisfy the above constraints. Replacing δ_j in the term at the left side of (19), we obtain the following

$$\sum_{j=1}^{L+1} \delta_j \mathbf{s}_{j,L} = \frac{1}{L+1}\sum_{j=1}^{L+1} \mathbf{s}_{j,L} = \frac{L}{L+1}\mathbf{s}_{i,L+1}, \tag{20}$$

where the second equality holds since we have $L+1$ elements to sum, each of which contains L '1' and one '0', and this '0' changes position with the different elements. The sum corresponding to each coordinate is then equal to L.
In order to better understand the result, we provide a geometric interpretation of the above lemma. We take the example given in the figure below. In this case we have $S_1 = \{(1,0);(0,1)\}$ and $S_2 = \{(1,1)\}$. Let $P_2 = (1,1)$ and $P_1 = (\frac{1}{2}, \frac{1}{2})$. Note that $P_2 \in S_2$ and P_1 is in the convex hull of S_1. We can express P_2 as $P_2 = \frac{2}{1}[\frac{1}{2}(1,0) + \frac{1}{2}(0,1)] = 2(\frac{1}{2}, \frac{1}{2}) = \frac{2}{1}P_1$. Thus, P_2 equals $\frac{2}{1}\times$ a specific point (P_1) in the convex hull of S_1.

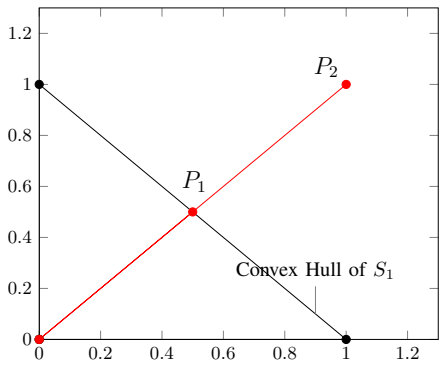

Figure 4: Example that illustrates the result of Lemma 3.

This completes the proof of Lemma 3. □

Using Lemma 3, a point $\mathbf{s}_{i,L+1}$ in S_{L+1} can be expressed in function of $L+1$ specific points in S_L as $\mathbf{s}_{i,L+1} = \frac{L+1}{L}\sum_{j=1}^{L+1}\delta_j \mathbf{s}_{j,L}$, which implies that

$$r_{L+1}\mathbf{s}_{i,L+1} = r_{L+1}\frac{L+1}{L}\sum_{j=1}^{L+1}\delta_j \mathbf{s}_{j,L} \tag{21}$$

By Lemma 1, we have $(L+1)r_{L+1} < Lr_L$ for $L \geq L_m$. We thus get

$$r_{L+1}\frac{L+1}{L}\sum_{j=1}^{L+1}\delta_j \mathbf{s}_{j,L} < r_L\frac{L}{L}\sum_{j=1}^{L+1}\delta_j \mathbf{s}_{j,L} = r_L\sum_{j=1}^{L+1}\delta_j \mathbf{s}_{j,L} \tag{22}$$

Note that the inequality operator in (22) can be used since the two compared points are on the same line (from the origin). Therefore, each point in R_{L+1} is inside the convex hull of R_L for $L \geq L_m$, since $r_{L+1}\mathbf{s}_{i,L+1} \in R_{L+1}$ and $r_L\sum_{j=1}^{L+1}\delta_j \mathbf{s}_{j,L}$ is in the convex hull of R_L. Consequently, all the points in R_{L+1} for $L \geq L_m$ (i.e. these points form $\bar{\mathcal{R}}$) are inside the convex hull of R_{L_m} which is a subset of $\mathcal{R}$.
In the following, we illustrate a geometric representation of this result for the case where $N = 2$ and $L_m = 1$. For this example, we have $\mathcal{R} = \{(0,0);(r_1,0);(0,r_1)\}$ and $\bar{\mathcal{R}} = \{(r_2,r_2)\}$. In addition, using Lemma 1 we can write $2r_2 < r_1$. We can easily notice that the set $\bar{\mathcal{R}}$ is inside the convex hull of $\mathcal{R}$.

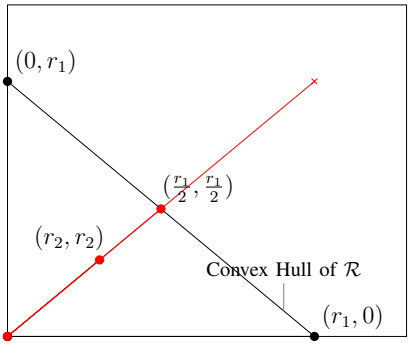

Figure 5: Example that shows the result of Lemma 2.

This completes the proof.

Appendix C
Proof of Theorem 1

First we prove that Λ_c is achievable. Indeed, a point $\mathbf{r}_c$ in Λ_c can be written as the convex combination of all the points in $\mathcal{R}$ as $\mathbf{r}_c = \sum_{i=1}^{|\mathcal{R}|} p_i \mathbf{r}_i$, where $\mathbf{r}_i$ represents a point in $\mathcal{R}$ and $\sum_{i=1}^{|\mathcal{R}|} p_i = 1$. Note that each point (decision) r_i represents a different scheduled subset of pairs. To achieve $\mathbf{r}_c$, it suffices to use a randomized policy that at the beginning of each timeslot selects decision r_i with probability p_i.

We then have to prove the converse, that is, if there exists a policy that stabilizes the system for a mean arrival rate vector $\mathbf{a}$, then $\mathbf{a} \in \Lambda_c$. To this end, assume that a policy π renders the system stable for a mean arrival rate vector $\mathbf{a}$. Thus, the system can be described as a Markov chain and since it is strongly stable it has a stationary distribution $\pi(\mathbf{q})$. Let $\mathcal{L}$ denote the set of users to be scheduled. Note that the scheduling decision depends on the queues states, and this dependency is shown by $\mathcal{L}(\mathbf{q})$. The mean service rate vector under π which stabilizes the system can then be expressed as the following

$$\mathbf{r}_s = \sum_{\mathbf{q}\in\mathbb{Z}_+^N}\pi(\mathbf{q})\mathbf{r}(\mathcal{L}(\mathbf{q})) = \sum_{\mathcal{L}}\mathbf{r}(\mathcal{L})\sum_{\mathbf{q}:\mathcal{L}(\mathbf{q})=\mathcal{L}}\pi(\mathbf{q}) > \mathbf{a}, \tag{23}$$

where the operator $>$ is component-wise.
By setting $p(\mathcal{L}) = \sum_{\mathbf{q}:\mathcal{L}(\mathbf{q})=\mathcal{L}}\pi(\mathbf{q})$ and noticing that the set of all possible decisions is nothing but $\mathcal{S}$ (or equivalently, $\mathcal{R}\cup\bar{\mathcal{R}}$), the mean service rate can be re-written as

$$\mathbf{r}_s = \sum_{\mathcal{L}}p(\mathcal{L})\mathbf{r}(\mathcal{L}) = \sum_{j=1}^{|\mathcal{S}|}p_j\mathbf{r}_j, \tag{24}$$

in which $\mathbf{r}_j$ is used to denote a point in $\mathcal{R}\cup\bar{\mathcal{R}}$.
Using the above expression, we can state that $\mathbf{r}_s$ is in the convex hull of $\mathcal{R}\cup\bar{\mathcal{R}}$. But, since $\bar{\mathcal{R}}$ is in the convex hull of $\mathcal{R}$ represented by Λ_c (see Lemma 2), we have $\mathbf{r}_s \in \Lambda_c$ and then $\mathbf{a} \in \Lambda_c$.

Appendix D
Proof of Proposition 1

We show that policy Δ^* stabilizes the system for all $\mathbf{a} \in \Lambda_c$ by proving that the corresponding Markov chain is positive recurrent. For this purpose, we use Foster's theorem. Define the quadratic Lyapunov function $Ly(\mathbf{q}) = \frac{1}{2}\mathbf{q}\cdot\mathbf{q}$, and consider the drift of this function under policy Δ^* as $Dr^{(\Delta^*)}(\mathbf{q})$. Thus, we have

$$\begin{aligned} &Dr^{(\Delta^*)}(\mathbf{q}) \\ &= \mathbb{E}\left[Ly\left(\mathbf{q}^{(\Delta^*)}(t+1)\right) - Ly\left(\mathbf{q}^{(\Delta^*)}(t)\right) \mid \mathbf{q}^{(\Delta^*)}(t) = \mathbf{q}\right] \\ &\leq \frac{N}{2}a_{max}^2 + \frac{N}{2}b_{max}^2 + \mathbf{q}\cdot\mathbf{a} - \mathbb{E}[\mathbf{q}\cdot\mathbf{B}^{(\Delta^*)}(t) \mid \mathbf{q}] \end{aligned} \tag{25}$$

where the last inequality holds since we have $\mathbb{E}[\mathbf{A}(t)\cdot\mathbf{A}(t)] \leq Na_{max}^2$, $\mathbb{E}[\mathbf{B}^{(\Delta^*)}(t)\cdot\mathbf{B}^{(\Delta^*)}(t)] \leq Nb_{max}^2$ and $Dr^{(\Delta^*)}(\mathbf{q}) \leq Dr^{(\Delta^*)}(\mathbf{q}) + \mathbb{E}[\mathbf{A}(t)\cdot\mathbf{B}^{(\Delta^*)}(t)]$.
Since $\mathbf{a}$ is in Λ_c, there exists an $\epsilon > 0$ such that the relation $\mathbb{E}[B_k^{(\Delta)}(t)] \geq a_k + \epsilon$ holds for all k (with $k = 1,...,N$), where Δ is a randomized policy that stabilizes the system. In addition, for every policy different from Δ^*, and consequently for Δ, we can write $\mathbb{E}[\mathbf{q}\cdot\mathbf{B}^{(\Delta^*)}(t) \mid \mathbf{q}] \geq \mathbb{E}[\mathbf{q}\cdot\mathbf{B}^{(\Delta)}(t) \mid \mathbf{q}]$ which results from the definition of Δ^*. Thus, we get

$$Dr^{(\Delta^*)}(\mathbf{q}) \leq \frac{N}{2}(a_{max}^2 + b_{max}^2) - \epsilon\sum_{k=1}^{N}q_k, \tag{26}$$

which implies that the Markov chain is positive recurrent, since the drift is negative in all except finite number of states [13]. Therefore, Δ^* stabilizes the system for all $\mathbf{a} \in \Lambda_c$. Hence the statement follows.

Appendix E
Computational Complexity Reduction

We start by analyzing the complexity of the policy Δ^* (i.e. max-weight policy). Because what we are looking for (using Δ^*) is the maximum, thus it takes $O(2^N)$ after computing all values $r(\|\mathbf{s}\|_1)\,\mathbf{s}\cdot\mathbf{q}(t)$ to find the maximum value (resp. the

corresponding argument). Note that for two fixed vectors we can compute this product in time $O(N)$. Thus we would have $O(N2^N)$ ignoring computing $r(\|\mathbf{s}\|_1)$ (can be done offline). We can notice that for large N this algorithm is of high computational complexity (CC).

This analysis corresponds to the classical implementation of the max-weight algorithm. However, in our case the implementation of this algorithm does not require all this complexity. This is due to the fact that all the active users have the same average transmission rate r. This structural property of Δ^* allows us to propose an equivalent reduced CC implementation of Δ^*, given by the following:

Algorithm 1

Initialize $L = 0$.
Sort the queues in a descending order.
for $l = 1 : 1 : N$ **do**
    Consider sum_l = sum of the first l queues.
    if $r_l\, sum_l > r_L\, sum_L$ **then**
        put $L = l$
    end if
end for
Schedule pairs corresponding to the first L queues.

The proposed algorithm depends essentially on two steps, the "sorting algorithm" and the "for loop" which need, respectively, $O(N \log N)$ and $O(\frac{N(N+1)}{2}) = O(N^2)$. Therefore, the computational complexity of the proposed algorithm is $O(N^2 + N \log N)$ which is very small compared to $O(N2^N)$ especially for large N.

Appendix F
Proof of Theorem 2

We start by proving the following result (related to Lemma 3) which will help us in the proof of Theorem 2.

Lemma 4. *Each point in S_L can be written as $\frac{L}{L-n}\times$ some point in the convex hull of S_{L-n}, for $1 \leq n < L$.*

Proof. From Lemma 3, a point in S_L can be written as $\mathbf{s}_{i,L} = \frac{L}{L-1}\sum_{i_1} \delta_{i_1,L-1}\mathbf{s}_{i_1,L-1}$. Also, the point $\mathbf{s}_{i_1,L-1}$ ($\in S_{L-1}$) can be expressed in function of some specific points in S_{L-2} as $\mathbf{s}_{i_1,L-1} = \frac{L-1}{L-2}\sum_{i_2} \delta_{i_2,L-1}\mathbf{s}_{i_2,L-2}$. Following this reasoning until index $L-n$, we get

$$\begin{aligned}\mathbf{s}_{i,L} &= \frac{L}{L-1}\sum_{i_1}\delta_{i_1,L-1}\frac{L-1}{L-2}\sum_{i_2}\delta_{i_2,L-2}\cdots \\ &\quad \cdots\frac{L-n+1}{L-n}\sum_{i_n}\delta_{i_n,L-n}\mathbf{s}_{i_n,L-n} \\ &= \frac{L}{L-n}\sum_{i}\delta_{i,L-n}\mathbf{s}_{i,L-n}, \end{aligned} \tag{27}$$

in which $\delta_{i,L-n}$ is function of $\delta_{i_1,L-1}...\delta_{i_n,L-n}$, and $\sum_i \delta_{i,L-n} = 1$ since $\sum_{i_j}\delta_{i_j,L-j} = 1$ for $j = 1, ..., n$. From (27) and the fact that the point $\sum_i \delta_{i,L-n}\mathbf{s}_{i,L-n}$ is in the convex hull of S_{L-n}, the desired result holds. □

Using the above lemma, a point in S_L can be written in function of some point in the convex hull of S_1 as $\frac{L}{1}\sum_i \delta_{i,1}\mathbf{s}_{i,1}$. Thus, a point in G_L can be expressed using some specific point in the convex hull of G_1 as $\frac{L}{1}r_L\sum_i \delta_{i,1}\mathbf{s}_{i,1}$. On the other hand, a point on the same line from the origin of point $\frac{L}{1}r_L\sum_i \delta_{i,1}\mathbf{s}_{i,1}$ and in the convex hull of J_1 can be expressed as $r_{\text{zf}}\sum_i \delta_{i,1}\mathbf{s}_{i,1}$. If $Lr_L > r_{\text{zf}}$, we can notice that point $\frac{L}{1}r_L\sum_i \delta_{i,1}\mathbf{s}_{i,1}$ is outside Λ_{zf}. Therefore, under this condition, we have that a part of the stability region of IA surpasses the stability region of TDMA-ZF. On the other side, the condition $Lr_L < r_{\text{zf}}$ ensure that the stability region of IA is entirely inside Λ_{zf}. This completes the proof.

Appendix G
Case of Multiple Modulations

Consider the case where we use D modulations, each of which corresponds to a rate R_j. These modulations are associated to D SINR targets represented by τ_n, for $n = 1, ..., D$. Without loss of generality, we can assume that $\tau_1 < \tau_2 < ... < \tau_D$ which implies that $R_1 < R_2 < .... < R_D$. Hence, for L scheduled users the average transmission rate per scheduled (active) user can be written as

$$\begin{aligned}\phi_L &= (1-L\theta)R_D\mathbb{P}\left\{\gamma_k^m \geq \tau_D \mid L\right\} \\ &\quad + (1-L\theta)\sum_{j=1}^{D-1} R_j\mathbb{P}\left\{\tau_j \leq \gamma_k^m \leq \tau_{j+1} \mid L\right\} \\ &= (1-L\theta)R_1\mathbb{P}\left\{\gamma_k^m \geq \tau_1 \mid L\right\} \\ &\quad + (1-L\theta)\sum_{j=1}^{D-1}(R_{j+1}-R_j)\mathbb{P}\left\{\gamma_k^m \geq \tau_{j+1} \mid L\right\}, \end{aligned} \tag{28}$$

where the last equality holds since $\mathbb{P}\left\{\tau_j \leq \gamma_k^m \leq \tau_{j+1}\right\} = \mathbb{P}\left\{\gamma_k^m \geq \tau_j\right\} - \mathbb{P}\left\{\gamma_k^m \geq \tau_{j+1}\right\}$.

To analyze stability for this case, we consider the total average rate which corresponds to multiply (28) by L. The only difference with the one-modulation case is that we have, instead of one optimal number of pairs, D optimal number of pairs due to D success probabilities. Every optimal value maximizes a concave function represented by $L(1-L\theta)\mathbb{P}\left\{\gamma_k^m \geq \tau_j \mid L\right\}$ (with $j = 1, ..., D$), for which the optimal value of L has already been derived earlier. Let L_{m1} denote the maximum among the D optimal numbers. Since for all $L > L_{m1}$ the total average rate is a decreasing function, we can characterize the stability region for this case using the following proposition

Proposition 3. *The stability region for the considered system using multiple modulations is given by*

$$\Lambda_m = \mathcal{CH}\left\{E_1, E_2, ..., E_{L_{m1}}\right\} \tag{29}$$

where $E_L = \{\phi_L\mathbf{s}, \forall\mathbf{s} \in S_L\}$.

The proof of this proposition is essentially the same as the proof of Theorem 1; thus, we omitted it for brevity. Notice that the max-weight policy described earlier can be adopted to achieve Λ_m. Hence, we can use Algorithm 1 (replace r_L with ϕ_L) to reduce the computational complexity of this policy. Finally, a comparison with TDMA-ZF can be done in a similar way as for the case with one modulation.